

1 **Role of time-averaging of eddy covariance fluxes on water use efficiency** 2 **dynamics of Maize crop**

3 Arun Rao Karimindla, Shweta Kumari, Saipriya SR, Syam Chintala*, and BVN Phanindra
4 Kambhammettu

5 Department of Civil Engineering, Indian Institute of Technology Hyderabad, Telangana, India.

6 *Corresponding author: E-Mail: ce22resch11012@iith.ac.in; Tel: +91 7997014429

7 **Abstract**

8 Direct measurement of carbon and water fluxes at high frequency makes eddy
9 covariance (EC) as the most preferred technique to characterize water use efficiency (WUE).
10 However, reliability of EC fluxes is largely hinged on energy balance ratio (EBR) and inclusion
11 of low-frequency fluxes. This study is aimed at investigating the role of averaging period to
12 represent EC fluxes and its propagation into WUE dynamics. Carbon and water fluxes were
13 monitored in a drip-irrigated Maize field at 10 Hz frequency and are averaged over 1, 5, 10,
14 15, 30, 45, 60, and 120 minutes considering daytime unstable conditions. Optimal averaging
15 period to simulate WUE fluxes for each growth stage is obtained by considering cumulative
16 frequency (Ogive) curves. A clear departure of EBR from unity was observed during dough
17 and maturity stages of the crop due to ignorance of canopy heat storage, low frequency flux
18 losses and inadequate averaging period. Deviation in representing water (carbon) fluxes
19 relative to the conventional 30 min average is within $\pm 3\%$ ($\pm 10\%$) for 10-120 min averaging
20 and is beyond $\pm 3\%$ ($\pm 10\%$) for other time-averages. Ogive plots conclude that optimal
21 averaging period to represent carbon, water and WUE fluxes is 15-30 min for 6th leaf and
22 silking stages, and is 45-60 min for dough and maturity stages. Dynamics of WUE considering
23 optimal averaging periods are in the range of ($\mu \pm \sigma$: 1.49 ± 0.95 , 1.37 ± 0.74 , 1.39 ± 0.79 , and
24 $3.06 \pm 0.69 \mu\text{mol mmol}^{-1}$ for the 6th leaf, silking, dough, and maturity stages respectively. Error
25 in representing WUE with conventional 30 min averaging is marginal ($< 1.5\%$) throughout the
26 crop period except for the dough stage (12.12%). We conclude that the conventional 30 min
27 averaging of EC fluxes is not appropriate for representing WUE throughout the crop period.
28 Our findings can help in developing efficient water management strategies by accurately
29 characterizing WUE fluxes from the EC measurements.

30 **Keywords:** Eddy covariance, Maize crop, Time-average, Energy balance ratio, Ogive
31 function, Water use efficiency.

32 **Research Highlights:**

- 33 1. The time-averages that yield most effective energy balance closure are identified as 45
34 and 60 minutes.
- 35 2. Insufficiently short time-averages such as 1 and 5 minutes, as well as excessively long-
36 time-averages such as 120 minutes, resulted in a high relative error in representing
37 carbon and water fluxes.
- 38 3. The conventional 30-minute averaging period proved to be insufficient in capturing
39 low-frequency fluxes, necessitating the use of longer averaging periods.
- 40 4. Different time averaging periods are to be considered to compute the EC fluxes
41 considering the crop growth stage.

42 **1.0 INTRODUCTION**

43 Water use efficiency (WUE) is an important eco-hydrologic trait relating two important
44 processes of plant metabolism namely carbon fixation (via photosynthesis) and water
45 consumption (via transpiration) (Bramley, 2013). The need for achieving food security with
46 diminishing water resources under changing climate has made WUE as the controlling
47 parameter in planning and design of irrigation strategies (Tang, 2015). Depending on the scale
48 of investigation, WUE can be quantified at: i) leaf, ii) plant, iii) ecosystem, or iv) regional
49 scales (Medrano, 2015). Of these, ecosystem WUE has taken precedence in irrigation and
50 agronomy due to: i) accurate and reliable measurement using micrometeorological techniques,
51 ii) ability to evaluate the role of various water conservation techniques on ecosystem
52 productivity, and iii) understand the relation between carbon and water cycles in response to
53 changes in climate (Tang, 2015; Tong, 2014).

54 Eddy covariance (EC) is a non-destructive, micrometeorological technique for direct
55 measurement of water vapour (H₂O) and carbon (CO₂) fluxes between vegetation and
56 atmosphere at high temporal frequency (Aubinet, 1999; Leclerc and Foken, 2014). EC method
57 precisely measures the overall transfer of heat, mass, and momentum between the earth's
58 surface (such as vegetation) and the atmosphere. This is achieved by estimating the covariance
59 of turbulent fluctuations in vertical wind (referred to as eddies) with respect to the specific flux
60 under consideration such as H₂O, CO₂, temperature. EC represents the scalar fluxes of interest

61 (representative of eco-hydrological processes) from a region upwind of the measurement
62 known as the footprint. At ecosystem scale, WUE is estimated as the ratio of net primary
63 product (NPP: proxy for photosynthesis) to evapotranspiration (ET: proxy for water
64 consumption) (Peddinti, 2020). WUE is a key eco-hydrologic trait that is used to analyse the
65 role of climate change, drought, deficit irrigation, and management strategies on ecosystem
66 productivity. Currently, EC is the most accurate and reliable method for estimating carbon and
67 water exchanges, hence WUE at ecosystem scale (Tong, 2009). A number of studies have
68 demonstrated the efficacy of EC in estimating WUE across a wide range of ecosystems (Tang,
69 2015; Tong, 2014; Wang, 2017). Error sources that affect the accuracy of EC fluxes are
70 grouped into: i) Unrepresentative (due to footprint heterogeneity, unsatisfied underlying
71 theory), ii) Measurement uncertainties (due to random errors, interference and contamination,
72 sensor drifts) and iii) Measurement biases in fluxes (tilt, frequency losses, air density
73 fluctuations etc). Despite improvements in measurement accuracy, data sampling, and
74 processing techniques, EC method still suffers from the drawback of lack of conservation
75 among the energy terms, resulting in energy balance closure (EBC) problem (Charuchittipan,
76 2014; Foken, 2011; Reed, 2018). Lack of EBC as observed in EC system is reported across
77 diverse ecosystems ranging from simple bare soils (Oncley, 2007), to homogeneous grasslands
78 (Twine, 2000), to heterogeneous croplands (Peddinti, 2020), to complex forest ecosystem
79 (Charuchittipan, 2014; Wilson, 2002). Apart from the errors associated with instrumentation,
80 measurement, and neglected energy sinks, lack of EBC at the EC sites is also attributed to the
81 omission of low frequency secondary circulations in the turbulent flux estimation (Wilson,
82 2002). This problem can be circumvented by choosing appropriate averaging period during
83 flux estimation, the selection of which is based on: i) 'ensemble block time-averaging method'
84 (Finnigan, 2003; Malhi, 2004; Sakai, 2001), and ii) 'Ogive method' (Berger, 2001).

85 A number of studies have highlighted the importance of averaging period in quantifying
86 the EC fluxes, with an objective to obtain optimal time-averaging period under various canopy
87 and surface roughness conditions. While smaller averaging periods (15-30 min) are suitable
88 for managed croplands, flux estimation from forest and tall canopies demand longer averaging
89 periods (60-120 min) due to the presence of large-sized, slow moving eddies (Finnigan, 2003;
90 Sakai, 2001; Sun, 2006). Zhang (2013) concluded that time-averaging of EC fluxes has to be
91 done in accordance with the observation scale. In an analysis of Chengliu riparian forest in
92 China, they found that lower time-averaging periods (15 min) are suitable for daily variation
93 of EC fluxes, whereas higher time-averaging periods (60 min) are suitable for long-term flux

94 computations. A similar observation was made by Lee (2004) over farmlands. In a wheat field
95 in Yucheng, China, 10 min and 30 min averaging periods were found suitable for diurnal and
96 long-term flux observations respectively. Flux observations over a Maize crop at Daxing
97 experimental station in China conclude that optimal time-averaging period has to be considered
98 in accordance with crop growth stage (Feng, 2017). However, they observed a marginal (< 3
99 %) error in representing the fluxes at conventional 30 min averaging relative to the optimal
100 averaging obtained for each growth stage.

101 Maize is the third most important cereal crop in India after rice and wheat, and accounts
102 for about 10 % of total food production in the country (Sharma, 2018; Ficci 2014). In spite of a
103 huge area under cultivation (9.4 MHa), high production (23 million tons), and enormous water
104 consumption (18 BCM), both crop productivity (2.5 t ha^{-1}) and crop water productivity (CWP)
105 (1.83 kg m^{-3}) of Indian Maize are far lower than corresponding world averages (Sharma, 2018).
106 Low CWP (hence, WUE) of Indian Maize can be attributed to: i) a high dependence (85 %) on
107 erratic, uncertain rainfall, ii) low adoption of hybrid varieties, iii) improper drainage facilities
108 leading to water logging, and iv) unscientific application of irrigation water without analysing
109 soil-water-crop interactions (Shankar, 2012). Thus, an accurate quantification of WUE and its
110 temporal variation during the crop cycle is essential for effective irrigation water management
111 of Maize crop (Medrano, 2015).

112 While the effect of time-averaging on carbon and water fluxes measured at EC sites is
113 reported, the effect on their interaction term, i.e. WUE, which is crucial in irrigation water
114 management is unexplored. Evaluation of time-averaging period on WUE dynamics is
115 necessary to understand the contribution of low and high frequency photosynthetic carbon and
116 evaporative water fluxes generated from various field management strategies. Also, most of
117 the EC flux studies are confined to data rich AmeriFLUX, EuroFLUX, and ChinaFLUX sites,
118 with limited focus to Indian fragmented croplands. This motivates the present study, and the
119 objectives of this study are as follows: i) investigate the role of time-averaging of EC fluxes on
120 EBR and WUE dynamics, ii) identify optimal averaging period to evaluate carbon and water
121 (hence, WUE) fluxes of Maize crop, and iii) investigate the association of carbon, water, and
122 WUE fluxes between multiple averaging periods. Results of this study can help in designing
123 efficient management strategies using EC datasets in response to changes in WUE during the
124 crop cycle.

125

126 2.0 MATERIALS AND METHODOLOGY

127 2.1 Site Description and Instrumentation

128 Controlled Maize plots situated at Professor Jaya Shankar Telangana State Agricultural
129 University (PJ TSAU), Hyderabad, Telangana, India (17°19'17" N, 78°24'35" E, 559 m above
130 sea level) forms the study area. The region is composed of red gravel to sandy loam soils with
131 field capacity and wilting point in the ranges of 17.92 - 19.56 % and 8.2 – 9.87% respectively.
132 As per Koppen-Geiger's classification, the region falls under tropical savanna climate zone
133 (Aw) characterized by long dry and short wet seasons (Kottek, 2006). Mean annual
134 precipitation of the region is 900 mm (IMD, 2019) with more than 80% occurring during the
135 monsoon months (Jun-Sep). Temperatures are high during summer (mean \pm standard deviation:
136 38.33 ± 2.12 °C) and low during winter (30 ± 2.20 °C) months. Humidity of the region varies
137 from 35% in summer to 73% in monsoon (CGWB, 2013). Mean seasonal wind speed is in the
138 range of 1.5 to 2.7 m/s (Peddinti, 2020). Hydro-geologically, the study area forms part of the
139 Deccan plateau characterized by multiple layers of solidified flood basalt resulting from
140 volcanic eruptions. Depth to groundwater ranges from 12 m (pre-monsoon) to 6 m (post-
141 monsoon) (CGWB, 2013).

142 Meteorological parameters and turbulent fluxes were obtained for one crop season, i.e.
143 26 May to 06 Sep, 2019 using an open path eddy covariance (EC) flux tower. The flux system
144 is composed of integrated CO₂/H₂O open-path gas analyzer and 3D sonic anemometer
145 (IRGASON-EB-NC, Campbell Sci. Inc., USA) to measure CO₂ and H₂O concentrations at 3
146 m above the canopy. Raw data was collected with a logger (CR1000, Campbell Sci. Inc., USA)
147 at 10 Hz frequency. Additionally, slow response meteorological variables including
148 precipitation (TE525-L-PTL, Tipping Bucket, Campbell Sci. Inc., USA), soil heat flux
149 (HFP01SC-L-PTL, Campbell Sci. Inc., USA), solar radiation (CNR 4, Campbell Sci. Inc.,
150 USA), and soil moisture (CS616-L-PT-L, Campbell Sci. Inc., USA) were obtained at 10 min
151 intervals.

152

153 2.2 Data Collection and Processing

154 Table 1 shows the phenological stages of the Maize crop in the study area (Soujanya,
155 2021). Additionally, leaf-area index (LAI) and mean plant height were monitored during the
156 crop cycle (Table 1). The LAI was measured using the plant canopy analyser, whereas the plant

157 height was measured using a ruler from the base of the plant to its crown. Maize crops of the
 158 experimental fields are sown on 25th May 2019 and harvested on 6th September 2019 with a
 159 base period of 104 days.

160 **Table 1:** Phenological growth stages and physical properties of the Maize crop

S. No.	Growth stage	Start date	End date	Period Length (days)	Leaf Area Index (m ² m ⁻²)	Plant height (cm)
1	6 th leaf	26/05/2019	12/06/2019	18	0.61	46.8
2	Silking	13/06/2019	19/07/2019	37	1.56	75.2
3	Dough	20/07/2019	12/08/2019	24	3.46	133
4	Maturity	13/08/2019	06/09/2019	25	3.03	134

161

162 Data from the EC system at 10 Hz frequency was converted to ASCII format using
 163 LoggerNet (4.3) software (Campbell Scientific Inc., Logan, Utah, USA), and further
 164 aggregated to various averaging periods (1, 5, 10, 15, 30, 45, 60, and 120 minutes). Post data
 165 processing was done using EddyPro post-processing software (version 7.0.8, LI-COR, USA).
 166 Primary corrections performed on the raw dataset include tilt corrections, turbulent
 167 fluctuations, density fluctuations, frequency corrections and quality checks. Tilt corrections
 168 were made by the double axis rotation method for each averaging period. Either block average
 169 method or linear trending method were considered to compute the turbulent fluctuations. Block
 170 averaging method was used for detrending the fluxes at 1, 5, 10, 30, 45, and 60 min averaging
 171 periods. Longer averaging periods (e.g. 120 min) has resulted in inconsistency in the obtained
 172 fluxes, which is a weakness of the block averaging (Renhua, 2005; Sun et al., 2006). Hence,
 173 linear trend removal method was used to compute the fluxes for 120 min averaging period.
 174 Density fluctuation corrections were done using Webb–Pearman–Leuning (WPL)
 175 method. Quality checks were performed following a flagging policy proposed by Mauder and
 176 Foken (2006) (0-1-2 system). Flag set to "0" corresponds to the best quality fluxes, "1"
 177 corresponds to fluxes acceptable for general analysis, and "2" corresponds to poor quality
 178 fluxes that should be removed from the dataset. The resulting fluxes may exhibit spikes,

179 discontinuity, randomness etc. There is a need to perform secondary corrections on the data
 180 that include flux spike removal (Vickers and Mahrt 1997), friction velocity corrections (to filter
 181 night time observations), gap filling and uncertainty analysis (Finkelstein, 2001), skewness &
 182 kurtosis removal, spectral corrections, and frequency corrections. To correct flux estimates for
 183 low and high frequency losses due to instrument setup, intrinsic sampling limits of the devices,
 184 and various data processing decisions, spectral corrections are performed. Additionally, slow
 185 sensor meteorological data obtained at 1 min interval were processed for different time-
 186 averaging periods using the EddyPro post-processing software (version 7.0.8, LI-COR, USA).

187

188 **2.3 Effect of time-averaging on EBR and EC fluxes**

189 Violation of law of conservation of energy resulting from the EC observed energy terms
 190 is referred as energy balance closure (EBC). The available energy ($R_n - G$) is generally higher
 191 than the turbulent fluxes ($H + LE$), resulting in a positive balance (Eshonkulov, 2019) where R_n ,
 192 G , H and LE correspond to net radiation, soil heat flux, sensible heat and latent heat
 193 respectively. Apart from instrument and measurement issues, this lack of energy closure is
 194 thought to be partly from averaging periods and coordinate systems (Finnigan, 2003; Finnigan,
 195 2004; Gerken, 2018). The energy closure fraction, commonly termed as energy balance ratio
 196 (EBR) is used to evaluate the quality of EC data by examining energy fluxes at the surface
 197 (Chen and Li 2012), given by:

$$198 \quad EBR = \frac{H + LE}{R_n - G} \quad (1)$$

$$199 \quad H = \rho_a C_p \overline{w' T'} \quad (2)$$

$$200 \quad LE = L_v \overline{w' \rho_v'} \quad (3)$$

201 where ρ_a is the air density; C_p is the specific heat of air, w' is the wind velocity fluctuation, T'
 202 is the temperature fluctuation, L_v is the latent heat of vaporization and ρ_v' is the H₂O gas
 203 concentration fluctuation.

204 EBR helps to determine the averaging period required to calculate H and LE fluxes over a
 205 range of landscapes (Chen and Li 2012). A high EBR ($EBR \geq 0.7$) ensures reliability of EC
 206 observations for use with flux estimation (Barr et al., 2006; Kidston et al., 2010).

207 Eddy fluxes are computed as the covariance between instantaneous deviation in vertical
208 wind speed (w') and scalar component of interest (s') from their respective means, given by

$$209 \quad F \approx \overline{\rho_a w' s'} \quad (4)$$

210 where $\overline{\rho_a}$ is the mean air density, and the overbar represents the time-average of eddy fluxes,
211 which is of interest in the present study. Depending on the scalar component considered (ex:
212 temperature, water vapour (H₂O), carbon dioxide (CO₂) concentration), corresponding eddy
213 fluxes (ex: sensible heat, latent heat, carbon flux) are computed as below.

$$214 \quad F_{CO_2} \approx \overline{\rho_a w' CO_2'} \quad (5)$$

$$215 \quad F_{H_2O} \approx \overline{\rho_a w' H_2O'} \quad (6)$$

216 Ecosystem WUE is then estimated as the ratio of daytime carbon (net primary product) to water
217 fluxes (evapotranspiration), observed considering daytime unstable atmospheric conditions
218 (08:00 am to 04:00 pm) given by:

$$219 \quad WUE = \frac{NPP}{ET} = \frac{F_{CO_2}}{F_{H_2O}} \quad (7)$$

220 Fluxes originating from real-world sites are composed of both high frequency (turbulence) and
221 low frequency (advection) fluctuations, with a spectral gap in between. Isolating local
222 turbulence component for use with flux studies is achieved by choosing an appropriate
223 averaging period, T_1 (typically 30 minutes) on fast response measurements operating at high
224 frequency T_2 (Manon and Kristian 2020). Optimal averaging period (T_1) should be long enough
225 to reduce random error (Berger, 2001) and short enough to avoid non-stationarity associated
226 with advection (Foken & Wichura, 1996). The flux estimates (eq. 2) are further decomposed
227 into frequency dependent contributions, known as co-spectra $C_{ows}(f)$ between vertical wind
228 velocity (w) and scalar of interest (s) for frequencies ' f ' (Manon and Kristian 2020). For an
229 accurate estimation of the flux, it is essential that the EC method is applied under conditions
230 where the flow is stationary, and all eddies carrying flux are sampled. Given that the flow
231 remains stationary, an 'Ogive' serves as a check for the essential requirement to sample all
232 scales carrying the flux. Ogive function is well proposed to check if all low frequency fluxes
233 are included in the turbulent flux measured with the EC method (Foken & Wichura, 1996;
234 Foken et al., 2005). It is used to investigate the energy balance losses caused by low frequency
235 fluxes. Ogive analysis is performed to investigate the flux contribution from each frequency

236 range and to arrive at most suitable averaging period to capture most of the turbulent fluxes
 237 (Desjardans, 1989; Charuchittipan, 2014). Ogive function thus provides the cumulative sum of
 238 co-spectral energy starting from the highest frequency, given by:

$$239 \quad \text{Og}_{\text{ws}}(f_0) = \int_{f_0}^{\infty} \text{Co}_{\text{ws}}(f) df \quad (8)$$

240 The point of convergence on the Ogive plot to an asymptote corresponds to optimal averaging
 241 period (T_1) for use with averaging of high frequency turbulence fluxes. In other words, the
 242 point at which the Ogive plot flattens out represents the optimal averaging period. A total of
 243 eight averaging periods, i.e., 1, 5, 10, 15, 30, 45, 60, and 120 minutes were considered to
 244 investigate the role of time-averaging on EBR, EC and WUE fluxes, and further to arrive at the
 245 optimum averaging period for use with WUE estimation. The biophysical and physiological
 246 characteristics such as plant height, crop water requirement, LAI, etc. changes with respect to
 247 the crop growth stage (Chintala et al., 2024) and have a significant effect on the EC fluxes.
 248 Since these factors vary over growth stages, time-averaging of EC fluxes is separated based on
 249 crop growth stage.

250

251 **2.4 Performance Evaluation**

252 The ability of various averaging periods to close the energy balance and compute the
 253 EC fluxes is evaluated using three goodness of fit indicators, namely: a) coefficient of
 254 determination (R^2), b) root mean squared error (RMSE), and c) relative error (RE). While R^2
 255 and RMSE aim to quantify the error in closing the energy balance, RE is aimed to compute the
 256 error in estimating EC fluxes with conventional 30 min averaging period relative to optimal
 257 averaging period.

258 Root mean square error (RMSE) measures overall accuracy in closing the energy balance for
 259 a given averaging period by penalizing large errors heavily, given by:

$$260 \quad \text{RMSE} = \left[\frac{\sum_{i=1}^n ((R_n - G)_i - (H + LE)_i)^2}{n} \right]^{0.5} \quad (9)$$

261 where n is the number of observations.

262 Coefficient of determination (R^2) and Pearson correlation coefficient (r) are the measures of
 263 the strength of linear association between turbulent fluxes and available energy, given by:

$$264 \quad (10)$$

$$R^2 = \left\{ \frac{\sum_{i=1}^n [(R_n - G)_i - \overline{(R_n - G)}] [(H + LE)_i - \overline{(H + LE)}]}{\sqrt{\sum [(R_n - G)_i - \overline{(R_n - G)}]^2 [(H + LE)_i - \overline{(H + LE)}]^2}} \right\}^2$$

$$r = \left\{ \frac{\sum_{i=1}^n [(R_n - G)_i - \overline{(R_n - G)}] [(H + LE)_i - \overline{(H + LE)}]}{\sqrt{\sum [(R_n - G)_i - \overline{(R_n - G)}]^2 [(H + LE)_i - \overline{(H + LE)}]^2}} \right\} \quad (11)$$

Relative error (RE) provides the disparity in the fluxes estimated with conventional (30 min) relative to the fluxes estimated with optimal averaging period, given by:

$$RE = \left[\frac{F_{opt} - F_{30min}}{F_{opt}} \right] \times 100 \quad (12)$$

where F_{opt} and F_{30} are the flux of interest considering optimal and conventional (30 min) averaging periods.

Averaging period corresponding to high R^2 (close to 1), low RMSE (close to zero) is considered to be the optimal choice in representing the EC fluxes.

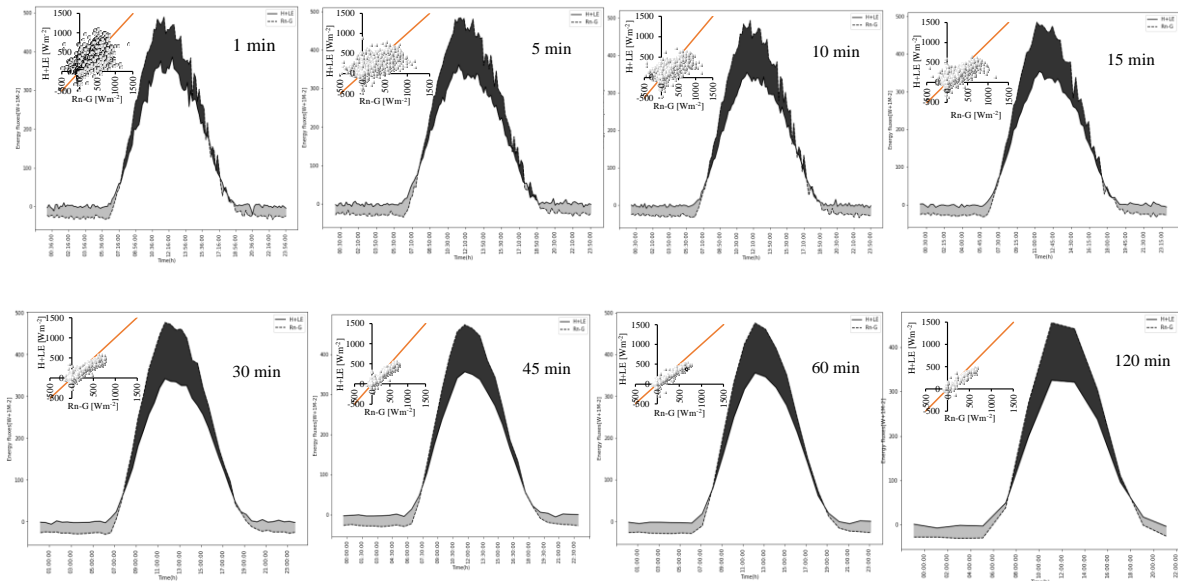
274

3.0 RESULTS AND DISCUSSION

3.1 Diurnal variations in energy balance components

To understand the energy variation in response to rapid changes in meteorological conditions, we analysed the diurnal variations in energy balance components. Figure 1 shows

279



280 **Figure 1:** Diurnal variations in energy balance components (available energy: R_n-G and turbulent fluxes:
 281 $H+LE$) during the crop cycle with different averaging periods. Inset: Scatter-plots between the two
 282 datasets.

283 the diurnal variations in available energy (R_n-G) and turbulent fluxes ($H+LE$) averaged over
 284 the crop cycle for various time-averages. The diurnal variations of (R_n-G) and ($H+LE$) are bell-
 285 shaped, with peak occurring at around noon ($480.16 \pm 14.15 \text{ Wm}^{-2}$, $356.23 \pm 18.51 \text{ Wm}^{-2}$)
 286 (Figure 1). The energy balance difference (shaded areas of the figure) is found to be positive
 287 ($76.88 \pm 43.14 \text{ Wm}^{-2}$) during daylight hours (08:00 am to 06:00 pm) and is negative ($-24 \pm$
 288 11.65 Wm^{-2}) for the remaining time. The vertical offset between the two curves, representing
 289 the residual of energy balance is highest around the noon ($142.39 \pm 19.42 \text{ Wm}^{-2}$), and is
 290 consistent between the averaging periods. For an average site-day, the cumulative energy
 291 balance difference was found to be constant with a mean of 1811 Wm^{-2} at all averaging periods.
 292 The cumulative energy balance difference is crossing the ‘zero’ line at around 11:30 am. The
 293 variation is rough at lower averaging periods due to a high sample size ($n= 10859$ at $T = 1$ min)
 294 and is gradually smoothed towards higher averaging periods ($n= 811$ at $T = 120$ min). The
 295 shorter averaging periods has introduced random uncertainty in the datasets during coordinate
 296 rotation correction. The slope of regression lines between ($H+LE$) and (R_n-G) considering all
 297 averaging periods are in the range of 0.59 to 0.71 with a mean of 0.65. The intercept is ranged
 298 from 19.01 to 31.56 Wm^{-2} . The best slope (≥ 0.70) and intercept ($\leq 20 \text{ Wm}^{-2}$) were achieved
 299 with 45 and 60 minutes averaging periods, which is consistent with literature (Gao, 2017;
 300 Leuning, 2012). This conclude that, longer averaging periods have a good closure over shorter
 301 averaging periods. The strength of linear association between (R_n-G) and ($H+LE$) around the
 302 best fit line, explained by r is high ($0.80 < r \leq 0.9$) at low averaging periods, i.e., 1, 5, 10
 303 minutes, and is very high ($r > 0.9$) for other averaging periods (Table 2). However, the departure
 304 of the data from 1:1 line is relatively low both at short and long averaging periods. Our findings
 305 show that averaging period has minimal influence in representing the energy balance terms.
 306 However, data scatter around 1:1 line is high for shorter time-averages due to large sample size
 307 and data randomness.

308 **Table 2:** Summary of linear regression parameters in closing the energy balance with different
 309 averaging periods.

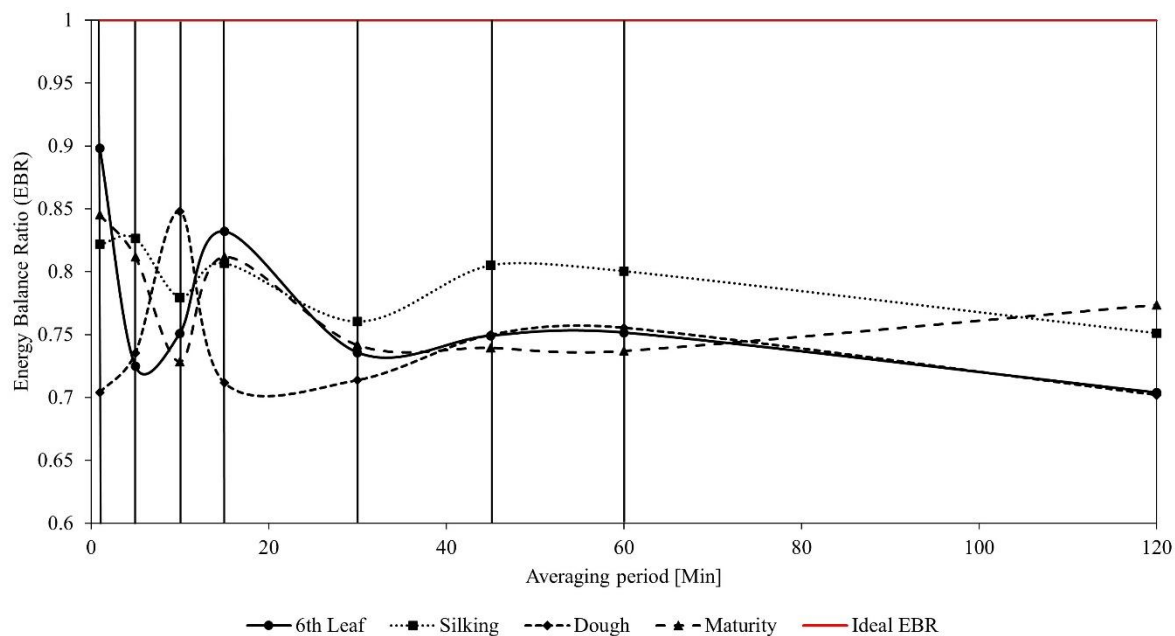
Averaging Period	Slope	R^2	Intercept (Wm^{-2})	r	N	RMSE (Wm^{-2})
------------------	-------	-------	-----------------------------------	-----	---	------------------------------

1min	0.63	0.66	30.31	0.81	10859	98.38
5min	0.59	0.74	31.56	0.86	10785	76.47
10min	0.60	0.80	28.94	0.90	10753	64.41
15min	0.63	0.84	26.56	0.92	7150	58.18
30min	0.66	0.93	20.49	0.96	3554	38.33
45min	0.70	0.94	19.99	0.97	2355	36.30
60min	0.71	0.94	19.01	0.97	1765	35.07
120min	0.67	0.93	20.77	0.96	811	39.95

310

311 3.2 Effect of averaging period on EBR and EC fluxes

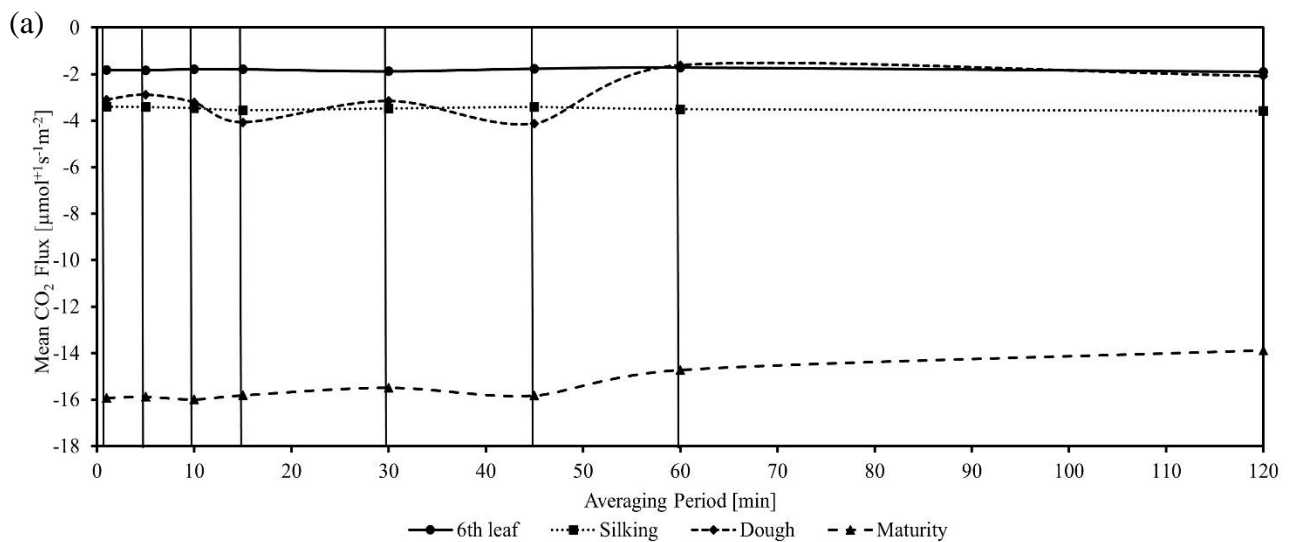
312 The variation in energy balance ratio (EBR) with averaging period for individual
 313 growth stages of the crop is presented in Figure 2. We observed a clear departure of EBR from



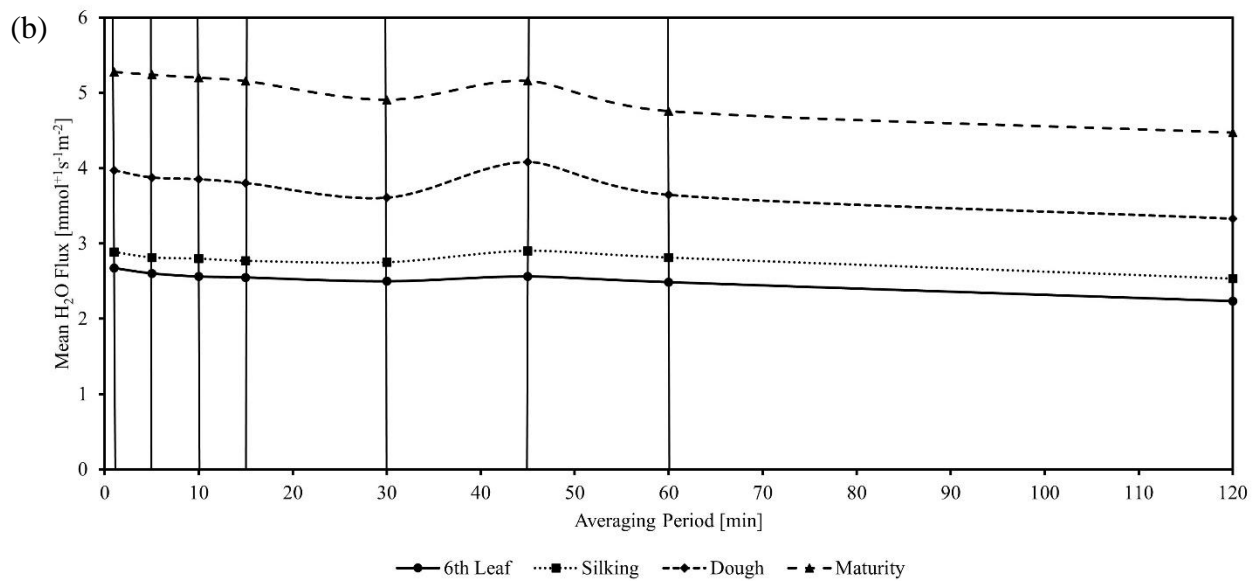
314

315 **Figure 2:** Variation in energy balance ratio (EBR) with averaging period for different growth stages. (Solid
 316 verticals from left to right correspond to the averaging periods of 1 min, 5 min, 10 min, 15 min, 30 min, 45
 317 min, 60 min, and 120 min respectively).

318 unity for all growth stages, particularly with dough and maturity stages due to ignorance of
 319 canopy heat storage, low frequency flux losses and inadequate averaging period (Meyers and
 320 Hollinger, 2004; Rahman et al., 2019). EBR is fluctuating between 0.70 and 0.90 at low (1 –
 321 30 min) averaging periods and is fairly constant (mean: 0.75) at high (≥ 30 min) averaging
 322 periods. Our reported values of EBR during the crop growth are within the typically found
 323 range of 0.65 to 1.2 for most of the crops (Feng, 2017; Finnigan, 2003; Wilson, 2002). The
 324 mean EBR with conventional 30 min averaging period is found to be 0.74, 0.76, 0.71, and 0.74
 325 during 6th leaf, silking, dough, and maturity stages respectively. Low EBR during the crop
 326 cycle can also be attributed to the ignorance of energy transport associated with large eddies
 327 from landscape heterogeneity (Meyers and Hollinger, 2004; Rahman et al., 2019). However,
 328 EC method assumes the landscape within the footprint of measurement to be flat and
 329 homogenous. We did not observe variations in optimal averaging time due to changes in wind
 330 speed and direction, hence meteorological conditions were not analysed in this study. Changes
 331 in daytime mean carbon and water fluxes with averaging period for different growth stages of
 332 the crop is shown in Figure 3. Carbon fluxes (sink) have a very low mean ($1.81 \mu\text{mol m}^{-2}\text{s}^{-1}$)
 333 during 6th leaf stage, low mean during silking ($3.48 \mu\text{mol m}^{-2}\text{s}^{-1}$) and dough ($3.03 \mu\text{mol m}^{-2}\text{s}^{-1}$)
 334 stages, and a high mean ($15.44 \mu\text{mol m}^{-2}\text{s}^{-1}$) during maturity stage.
 335



336



337

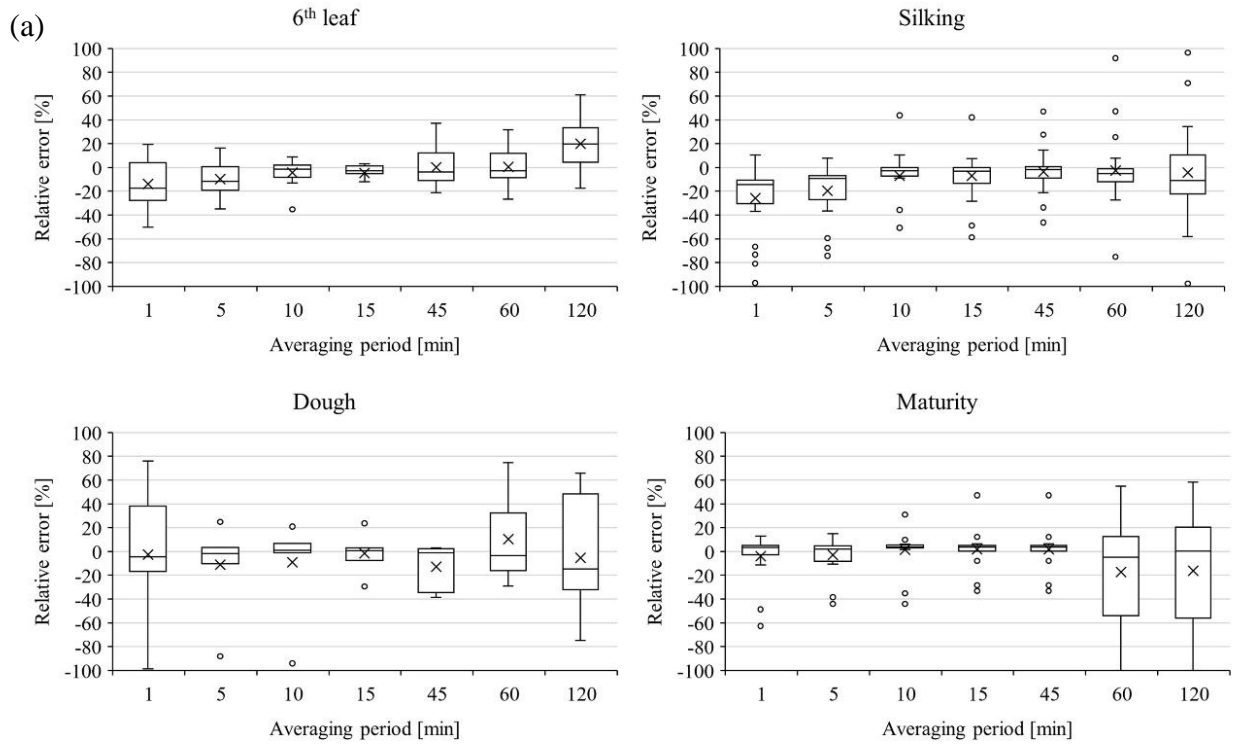
338 **Figure 3. (a)** Variation in mean carbon fluxes with averaging period for different growth stages. **(b)**
 339 Variation in mean water fluxes with averaging period for different growth stages (Solid verticals from left
 340 to right correspond to the averaging periods of 1 min, 5 min, 10 min, 15 min, 30 min, 45 min, 60 min, and
 341 120 min respectively).

342 Mean carbon fluxes during 6th leaf and silking stage are mostly unaffected by averaging period.

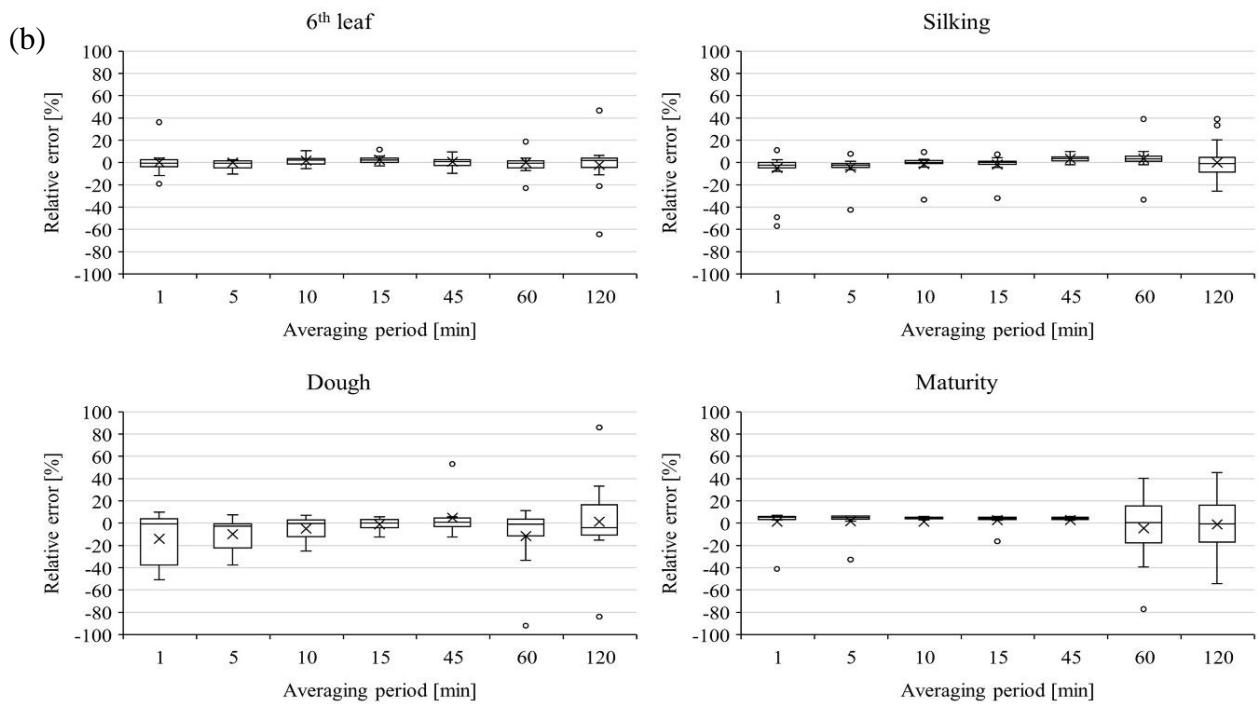
343 We observed a gradual increase in water vapour fluxes during the crop cycle from 6th leaf ($2.52 \pm 0.13 \text{ mmol s}^{-1}\text{m}^{-2}$) to maturity ($5.02 \pm 0.29 \text{ mmol s}^{-1}\text{m}^{-2}$). From the mean CO₂ and H₂O flux
 344 dynamics, it is observed that the drip irrigated Maize crop is acting as a carbon sink in the entire
 345 crop season especially in the latter stages of the crop i.e. maturity stage with a mean of $15.44 \mu\text{mol m}^{-2}\text{s}^{-1}$. This is clearly evident from the increasing trend of LAI and plant height during
 346 the crop season. Such an increase is highlighted by previous studies of Guo et al., 2021. At the
 347 same time, mean H₂O fluxes were increased towards the end of crop growing season due to
 348 increased crop water demand. As the averaging period is increased, the mean water vapour flux
 349 is decreased, with an exception at 45 min averaging period. Deviation in representing carbon
 350 and water fluxes at different averaging periods, relative to the conventional 30 min averaging
 351 period i.e. relative error (RE) is presented in Figure 4. The RE is obtained by considering daily
 352 averages in the deviations for each growth stage. During 6th leaf and silking stages, RE in
 353 estimating carbon fluxes is high ($\sim -15\%$) with low averaging periods, and is gradually
 354 diminishing towards higher averaging periods, with an exception at very high (120 min)
 355 average period. For dough and maturity stages, RE is found to be significant with higher
 356 averaging periods (60-120 min). RE in estimating water vapour fluxes is found to be
 357 insignificant at all averaging periods for the 6th leaf and silking stages. However, dough and
 358 maturity stages have shown a large variation in RE considering either too-short (1, 5 min) or
 359
 360

361 too-long (60, 120 min) time averages. A high variation in RE for time scales larger than 45 min
 362 indicate the effects of sub mesoscale (non-turbulent) motions. Hence, 45 min average period
 363 can be considered as optimal in isolating the turbulence components for use with flux
 364 representation.

365



366



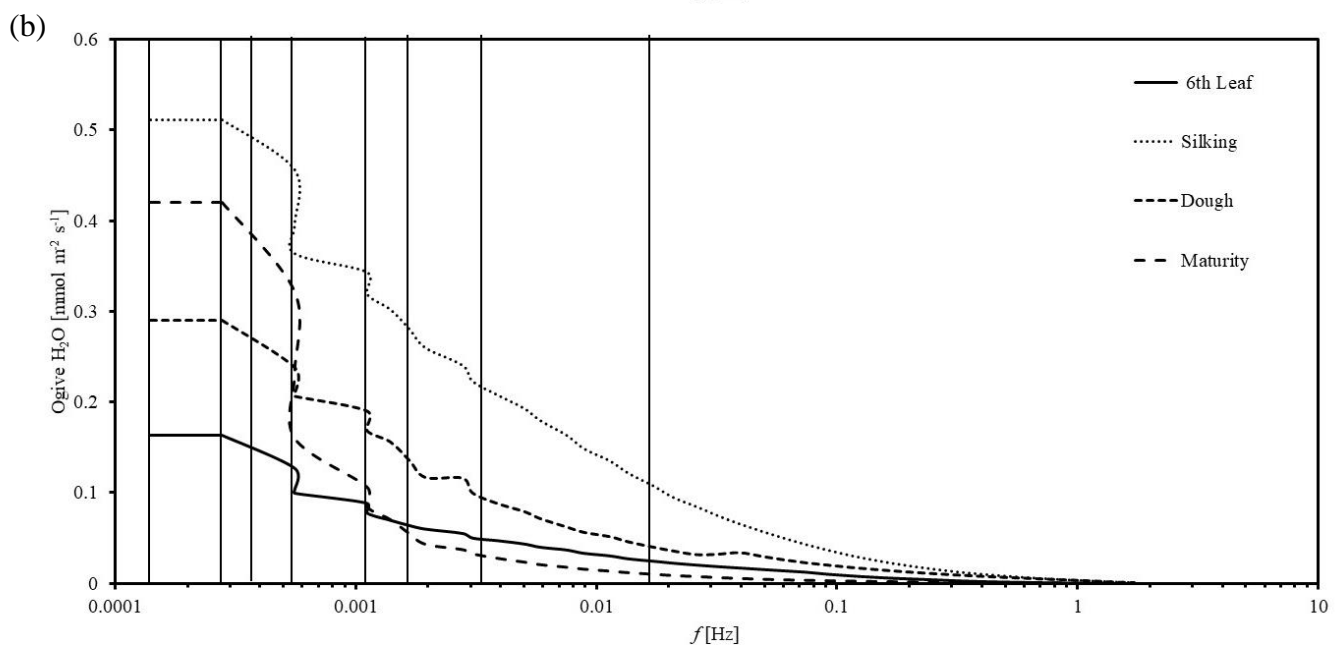
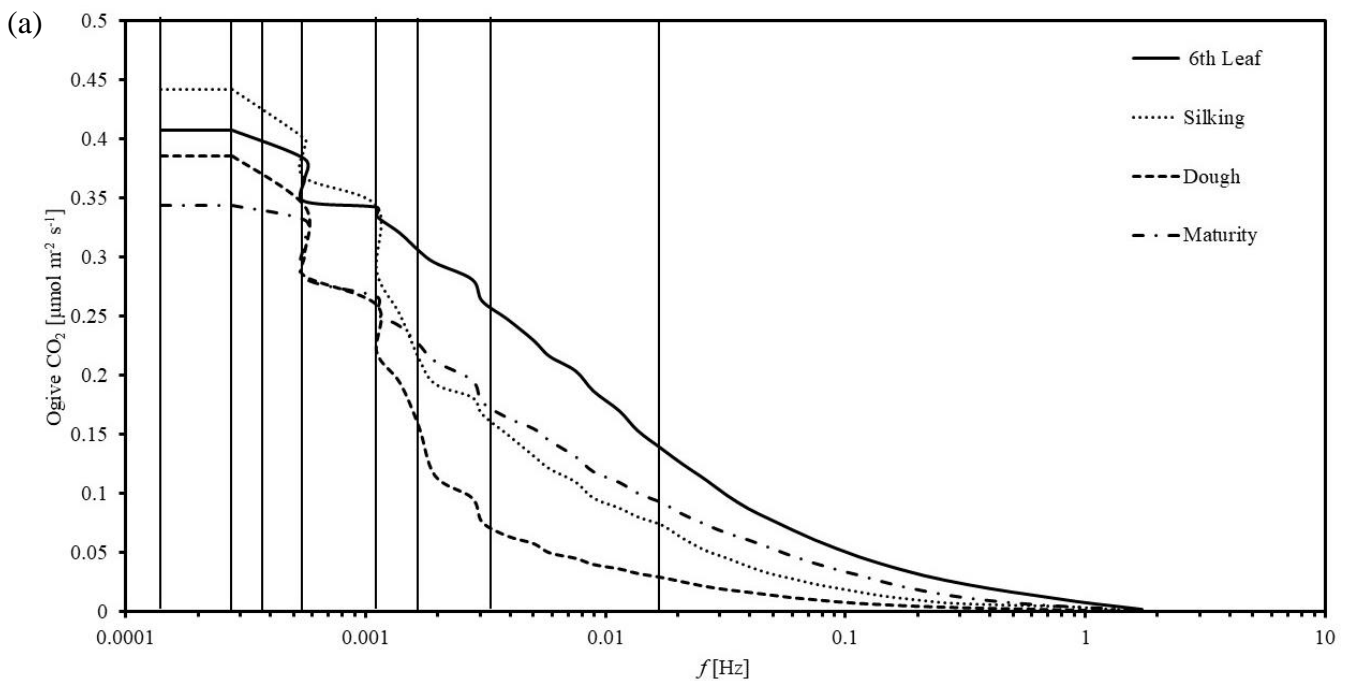
367

368 **Figure 4. (a)** Whisker plots showing the distribution of error in estimating carbon fluxes with various
 369 averaging periods relative to the conventional 30 min averaging. **(b)** Whisker plots showing the distribution
 370 of error in estimating water fluxes with various averaging periods relative to the conventional 30 min
 371 averaging.

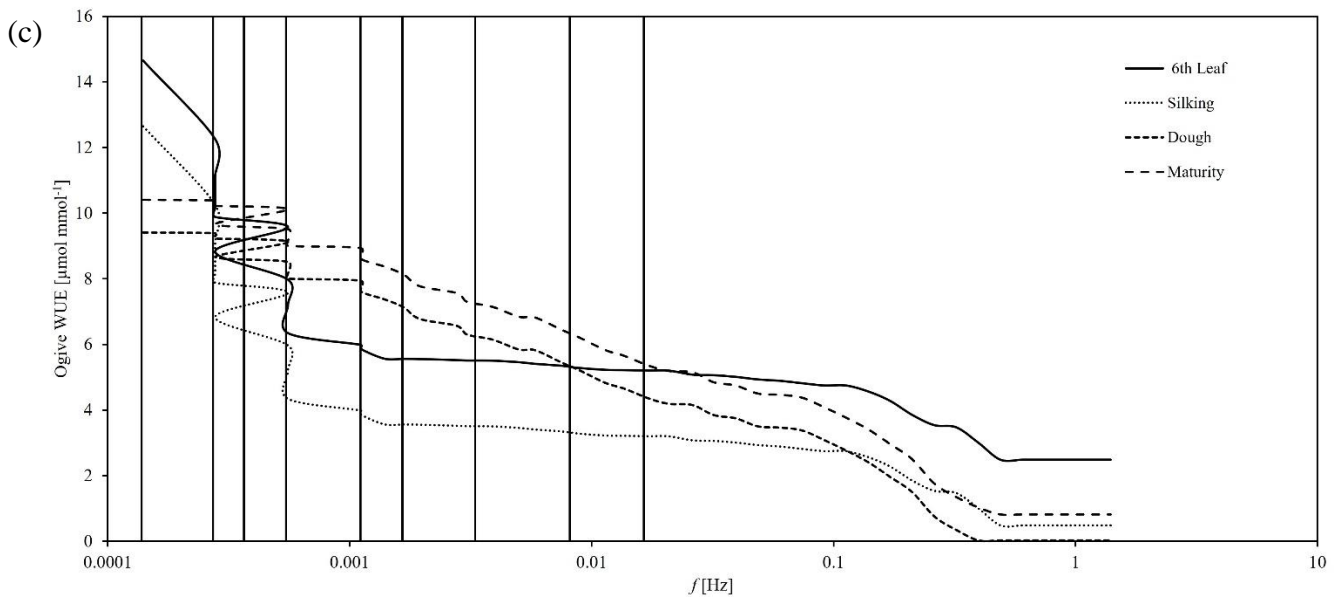
372

373 3.3 Selection of Optimal averaging period

374 Ogive functions representing the cumulative integral of the co-spectral energy starting
 375 with highest frequency, i.e., 0.016 Hz ($T = 1$ min) for carbon, water, and WUE fluxes are
 376 presented



378



379

380 **Figure 5.** (a) Ogive plots of carbon fluxes for different growth stages of the Maize crop. (b) Ogive plots of
 381 water fluxes for different growth stages of the Maize crop. (c) Ogive plots of water use efficiency for
 382 different growth stages of the Maize crop. (Solid verticals from left to right extremes correspond to the
 383 averaging periods of 120 min, 60 min, 45 min, 30 min, 15 min, 10 min, 5 min and 1 min respectively).

384

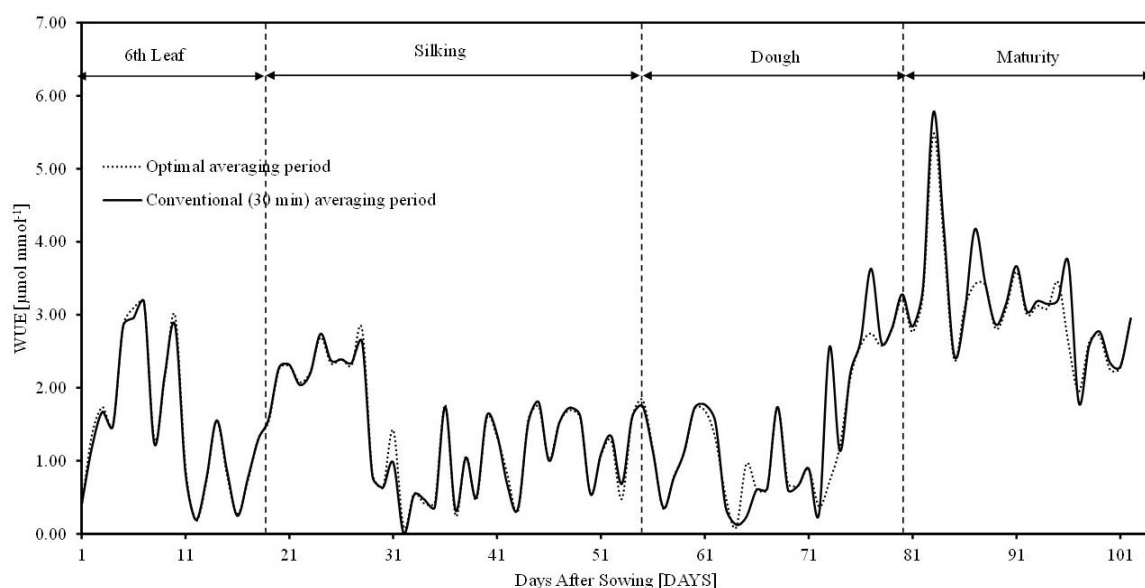
385 in Figure 5. Shorter time periods corresponding to daytime unstable atmospheric conditions
 386 (08:00 am to 04:00 pm) for various growth stages were investigated. Ogive plots of carbon
 387 fluxes for 6th leaf and silking stages showed an increasing trend up to 0.011 Hz (15 min) and
 388 remained fairly constant before 0.0055 Hz (30 min). This concludes that whole turbulent
 389 spectrum can be covered with 15 to 30 min averaging, with negligible flux contribution from
 390 longer frequencies. Ogive plots of carbon fluxes for dough and maturity stages showed a
 391 continuous increasing trend without a defined plateau (horizontal asymptote) in between. This
 392 conclude that the conventional 30 min averaging period is inadequate to capture the low
 393 frequency fluxes, thus demanding for higher averaging periods. We observed a similar
 394 behaviour with water fluxes (Figure 5b). The flat part of the Ogive curve representing the
 395 optimal averaging period was found to vary across the crop cycle. While 15-30 min time-
 396 average is suitable for aggregating the EC fluxes during 6th leaf and silking stages, 45-60 min
 397 averaging is more appropriate for dough and maturity stages. Similar to carbon and water
 398 fluxes, the Ogive plots for WUE were presented in Figure 5c. From this, it is observed that the
 399 flat part of Ogive is achieved at 15 min time average period for the stages of 6th leaf and silking
 400 and 45 min time average for the dough and maturity stages which is similar to the carbon and
 401 water fluxes. This concludes that the WUE co-spectrum followed a similar behaviour as its
 402 individual fluxes i.e. carbon and water fluxes in achieving optimal time averages. The crop
 403 biophysical factors like LAI and plant height are minimum during 6th leaf and silking stages

404 contributes low quantity of CO₂ and H₂O fluxes (refer figure 3a & 3b) whereas they are
 405 maximum in the later stages of the crop i.e., dough and maturity contributing to high quantities
 406 of CO₂ and H₂O fluxes (refer figure 3a & 3b). Our results are in accordance with the previous
 407 studies of Fong et al., 2020 on Cotton, where the responses in NPP and ET were related
 408 seasonally to plant growth stages. The previous studies on various crops revealed that the NPP
 409 and ET fluxes were initially low in the early stages and increases towards maturity stage due
 410 to crop phenology and management practices. To capture these low quantity fluxes, low
 411 averaging periods i.e., 15 min is sufficient, whereas 45 min time-averaging period can capture
 412 high quantity fluxes that are prevalent during later growth stages of the crop. As the crop
 413 characteristics are dependent on crop growth stages, a single time-averaging period is not
 414 appropriate to capture the dynamics of CO₂ and H₂O fluxes as well their ratio, WUE. This
 415 clearly demonstrates that, as the plant achieves its higher stage, flux contribution from low-
 416 frequency components becomes more predominant. Very low averaging periods (ex: 1 min, 5
 417 min) were found unsuitable to capture low-frequency flux components, which is in agreement
 418 with literature (Feng, 2017).

419

420 3.4 Dynamics of Water use efficiency

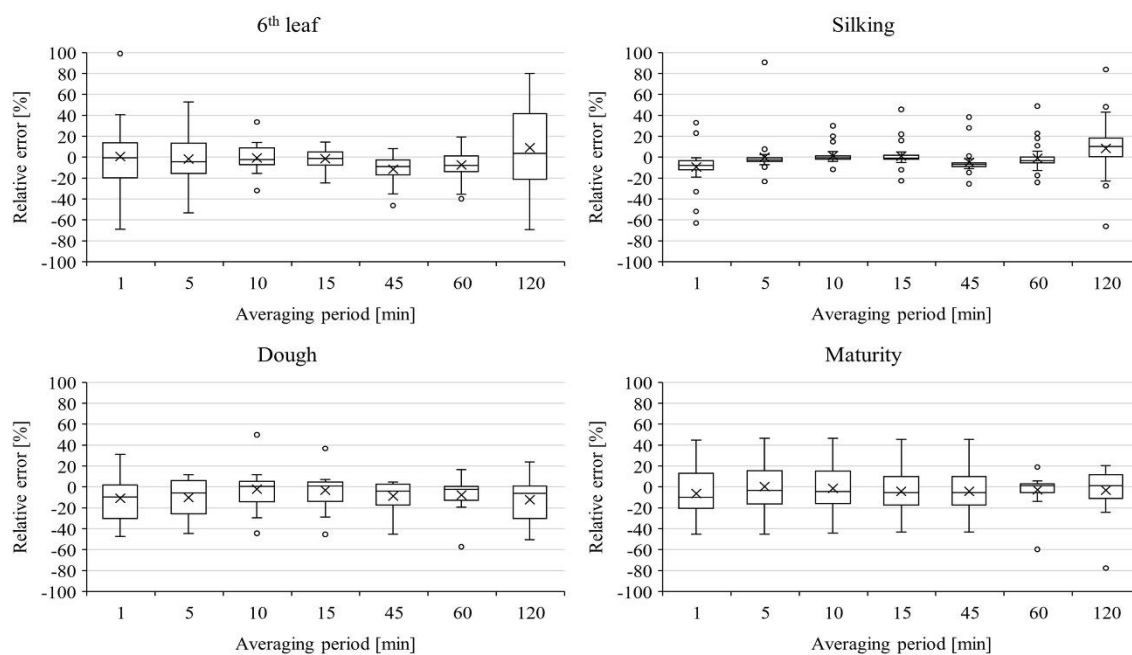
421 Daily means of water use efficiency (WUE) estimated with conventional 30 min and
 422 growth specific optimal averaging periods is presented in Figure 6. Mean WUE fluxes for 6th



423

424 **Figure 6:** Seasonal variations in daily mean WUE fluxes obtained with conventional 30 min (solid) and
 425 optimal averaging periods (dotted) during the crop cycle.

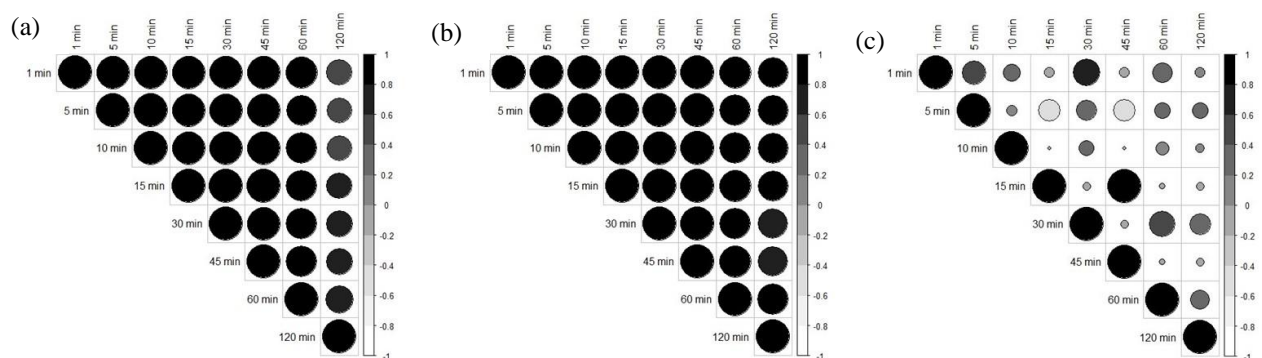
426 leaf, silking, dough and maturity stages with conventional 30 min averaging are 1.48, 1.36,
 427 1.38 and 3.184 $\mu\text{mol mmol}^{-1}$ respectively. Corresponding fluxes with stage specific optimal
 428 averaging periods are 1.49, 1.37, 1.39 and 3.06 $\mu\text{mol mmol}^{-1}$ respectively. Error in estimating
 429 mean daily WUE fluxes with 30 min averaging is very low ($< 1.45\%$) during 6th leaf and silking
 430 stages, low (8.56 to 9.04 %) during maturity stage, and is moderate (11.84 to 12.12 %) during
 431 dough stage. This conclude that, choice of optimal averaging period is more crucial for late
 432 stage growth periods of the crop. Distribution of error in estimating WUE fluxes with various
 433 averaging periods relative to conventional 30 min average period (RE) is presented in Figure
 434 7. A close to zero RE with all averaging periods during 6th leaf and silking stages conclude
 435 that, choice of averaging period has insignificant role in estimating the WUE fluxes,
 436 particularly during early growth stages. A slightly high RE ($\sim -5.4\%$) during dough and
 437 maturity stages conclude that, choice of averaging period matters for WUE estimation during
 438 late stage periods. Hence, conventional 30 min averaging period can be considered for
 439 estimating WUE fluxes during 6th leaf and silking stages, whereas optimal averaging period
 440 need to be considered for estimating WUE fluxes during dough and maturity stages.
 441 Correlation charts showing the linear association considering daily means of carbon, water,
 442 and WUE fluxes at different averaging periods is represented in Figure 8. For ease with
 443 comparison, data for the entire crop cycle was considered. Linear association



444

445 **Figure 7:** Whisker plots showing the distribution of error in estimating WUE fluxes with various averaging
 446 periods relative to the conventional 30 min averaging.

447 between any two averaging periods is positive ($r > 0.56$) for carbon and water fluxes. Except
 448 with 120 min time-averaging, all other averaging periods are strongly correlated ($r > 0.87$) with
 449 30 min averaging period. Surprisingly, a poor linear association in WUE fluxes was observed
 450 between any two averaging periods, which is attributed to a larger variation in individual WUE
 451 fluxes between averaging periods. However, the corresponding individual carbon and water
 452 fluxes have recorded low variations between time averages. This conclude that, the need for
 453 optimal averaging period is more crucial in representing WUE fluxes rather than individual
 454 carbon and water fluxes. Our findings can improve representation of WUE fluxes using EC
 455 data, thereby help in developing efficient water management strategies in response to WUE
 456 changes.



457
 458 **Figure 8:** Correlation charts showing the linear association of (a) Carbon fluxes, (b) Water fluxes, and (c)
 459 WUE fluxes estimated with different averaging periods. Circle size represents the correlation magnitude
 460 and the color sign from white to black represents the negative to positive correlations respectively.

461

462 4.0 CONCLUSIONS

463 This study explores the effect of averaging period of EC fluxes on EBR dynamics and
 464 WUE in semi-arid Indian conditions. The proposed methodology was applied on drip-irrigated
 465 Maize field for one crop period (May-Sept 2019). Major findings of this study are:

- 466 • EBR was found to vary marginally at low averaging periods and less significant during
 467 higher averaging periods.
- 468 • With reference to conventional 30 min averaging period, relative error is within 12%
 469 for 10-45 min averaging periods for carbon fluxes and is within 5% for 15-45 averaging
 470 periods for water fluxes.
- 471 • From Ogive analysis we found the optimal averaging period as 15 - 30 min for the 6th
 472 leaf, and silking stages, and as 45 – 60 min for the dough and maturity stages.

- 473 • The mean carbon fluxes are increasing from $1.81 \mu\text{mol}^+\text{m}^{-2}\text{s}^{-1}$ (6th leaf stage) to 15.44
474 $\mu\text{mol}^+\text{m}^{-2}\text{s}^{-1}$ (maturity stage) which indicates that carbon sink is a function of crop
475 growth period. In case of water fluxes, it increased from $2.52 \text{mmol}^+\text{m}^{-2}\text{s}^{-1}$ (6th leaf
476 stage) to $5.02 \text{mmol}^+\text{m}^{-2}\text{s}^{-1}$ (maturity stage). Variation of carbon and water fluxes are
477 directly influencing WUE dynamics.
- 478 • The variation in WUE was increased subsequently with the plant growth and achieved
479 its maximum value of $5.17 \mu\text{mol mmol}^{-1}$ in between dough to maturity stages which
480 concludes that, crop consumes more carbon than water as the crop period progresses.
- 481 • The correlation between CO_2 and H_2O fluxes for all averaging periods was found to be
482 high. However, WUE, which is calculated as the ratio of CO_2 and H_2O fluxes, is not
483 following the same pattern. While 45 min and 15 min averaged WUE exhibits a good
484 correlation, 30 min averaged WUE is not correlated with other averaging periods.
485 Averaging period is found to be an influencing factor in controlling WUE, hence should
486 be considered with caution during the crop growth.

487 This study is limited to understand the role of different time-averaging periods on EC observed
488 carbon, water fluxes as well as EC derived WUE fluxes contributed by homogeneous Maize
489 crop which is having relatively smaller flux footprint in an unstable atmospheric condition.
490 Study findings can help to accurately characterise WUE of Maize crop considering growth
491 stages for effective implementation of irrigation strategies.

492

493 **Acknowledgments**

494 The authors acknowledge the anonymous reviewers for their insightful comments. This
495 research evolved as an extension of a term project in CE6520-Irrigation Water Management
496 course at IIT Hyderabad.

497

498 **Data Availability Statement:**

499 All footprint climatologies, site-level data files, and supplementary material can be accessed
500 via the Zenodo Data Repository (<https://zenodo.org/badge/latestdoi/528291820>)
501 (Shweta07081992, 2022)

502

503 **Author Contribution:**

504 **Arun Rao Karimindla**: Data processing and Analysis, Writing- Original draft. **Shweta**
 505 **Kumari**: Conceptualization, Methodology, Project Supervision. **Saipriya SR**: Data processing
 506 Analysis, and Writing- Original draft. **Syam Chintala**: Data processing and Analysis, Writing-
 507 Original draft, Reviewing and Editing. **BVN Phanindra Kambhammettu**: Project
 508 Administration, Writing- Reviewing and Editing.

509

510 **Competing interests:**

511 The authors declare that they have no known competing interests or personal relationships that
 512 could have appeared to influence the work reported in this paper.

513

514 **5.0 REFERENCES**

515 Barr, A. G., Morgenstern, K., Black, T. A., McCaughey, J. H., & Nesic, Z. (2006). Surface
 516 energy balance closure by the eddy-covariance method above three boreal forest stands
 517 and implications for the measurement of the CO₂ flux. *Agricultural and Forest*
 518 *Meteorology*, 140(1–4), 322–337. <https://doi.org/10.1016/j.agrformet.2006.08.007>

519 Bramley, H., Turner, N. C., & Siddique, K. H. M. (2013). Water Use Efficiency. In C. Kole
 520 (Ed.), *Genomics and Breeding for Climate-Resilient Crops: Vol. 2 Target Traits* (pp.
 521 225–268). Springer Berlin Heidelberg. https://doi.org/10.1007/978-3-642-37048-9_6

522 Berger, B. W., Davis, K. J., Yi, C., Bakwin, P. S., & Zhao, C. L. (2001). Long-term carbon
 523 dioxide fluxes from a very tall tower in a northern forest: Flux measurement
 524 methodology. *Journal of Atmospheric and Oceanic Technology*, 18(4), 529–542.

525 Central Ground Water Board. (2015). Annual Report 2013.
 526 https://cgwb.gov.in/old_website/Annual-Reports/Annual-Report-2013-14.pdf

527 Charuchittipan, D., W. Babel, M. Mauder, J. P. Leps, and T. Foken, 2014: Extension of the
 528 Averaging Time in Eddy-Covariance Measurements and Its Effect on the Energy
 529 Balance Closure. *Boundary-Layer Meteorol.*, **152**, 303–327,
 530 <https://doi.org/10.1007/s10546-014-9922-6>.

531 Chen, Y. Y., and M. H. Li, 2012: Determining adequate averaging periods and reference
 532 coordinates for eddy covariance measurements of surface heat and water vapor fluxes
 533 over mountainous terrain. *Terr. Atmos. Ocean. Sci.*, **23**, 685–701,

- 534 [https://doi.org/10.3319/TAO.2012.05.02.01\(Hy\)](https://doi.org/10.3319/TAO.2012.05.02.01(Hy)).
- 535 Chintala, S., Karimindla, A. R., & Kambhammettu, B. V. N. P. (2024). Scaling relations
536 between leaf and plant water use efficiencies in rainfed Cotton. *Agricultural Water*
537 *Management*, 292, 108680. <https://doi.org/10.1016/j.agwat.2024.108680>
- 538 Desjardins, R. L., MacPherson, J. I., Schuepp, P. H., & Karanja, F. (1989). An evaluation of
539 aircraft flux measurements of CO₂, water vapor and sensible heat. *Boundary-Layer*
540 *Meteorology*, 47(1), 55–69. <https://doi.org/10.1007/BF00122322>
- 541 Eshonkulov, R., and Coauthors, 2019: Evaluating multi-year, multi-site data on the energy
542 balance closure of eddy-covariance flux measurements at cropland sites in southwestern
543 Germany. *Biogeosciences*, **16**, 521–540, <https://doi.org/10.5194/bg-16-521-2019>.
- 544 Feng, J., B. Zhang, Z. Wei, and D. Xu, 2017: Effects of Averaging Period on Energy Fluxes
545 and the Energy-Balance Ratio as Measured with an Eddy-Covariance System.
546 *Boundary-Layer Meteorol.*, **165**, 545–551, <https://doi.org/10.1007/s10546-017-0284-8>.
- 547 Ficci, 2014: Maize in India. *India Maize Summit '14*, 1–32.
- 548 Finkelstein, P. L., & Sims, P. F. (2001). Sampling error in eddy correlation flux
549 measurements. *Journal of Geophysical Research*, 106, 3503–3509.
550 <https://api.semanticscholar.org/CorpusID:128980052>
- 551 Finnigan, J. J., 2004: A re-evaluation of long-term flux measurement techniques part II:
552 Coordinate systems. *Boundary-Layer Meteorol.*, **113**, 1–41,
553 <https://doi.org/10.1023/B:BOUN.0000037348.64252.45>.
- 554 Finnigan, J. J., R. Clement, Y. Malhi, R. Leuning, and H. A. Cleugh, 2003: Re-evaluation of
555 long-term flux measurement techniques. Part I: Averaging and coordinate rotation.
556 *Boundary-Layer Meteorol.*, **107**, 1–48, <https://doi.org/10.1023/A:1021554900225>.
- 557 Foken, T., and B. Wichura, 1996: Tools for quality assessment of surface-based flux
558 measurements. *Agric. For. Meteorol.*, **78**, 83–105, [https://doi.org/10.1016/0168-](https://doi.org/10.1016/0168-1923(95)02248-1)
559 [1923\(95\)02248-1](https://doi.org/10.1016/0168-1923(95)02248-1).
- 560 Foken, T., Göockede, M., Mauder, M., Mahrt, L., Amiro, B., & Munger, W. (2005). Post-
561 Field Data Quality Control BT - Handbook of Micrometeorology: A Guide for Surface
562 Flux Measurement and Analysis (X. Lee, W. Massman, & B. Law, Eds.; pp. 181–208).
563 Springer Netherlands. https://doi.org/10.1007/1-4020-2265-4_9

- 564 Foken, T., M. Aubinet, J. J. Finnigan, M. Y. Leclerc, M. Mauder, and K. T. Paw U, 2011:
565 Results of a panel discussion about the energy balance closure correction for trace gases.
566 *Bull. Am. Meteorol. Soc.*, **92**, <https://doi.org/10.1175/2011BAMS3130.1>.
- 567 Fong, B. N., Reba, M. L., Teague, T. G., Runkle, B. R. K., & Suvočarev, K. (2020). Eddy
568 covariance measurements of carbon dioxide and water fluxes in US mid-south cotton
569 production. *Agriculture, Ecosystems and Environment*, 292.
570 <https://doi.org/10.1016/j.agee.2019.106813>
- 571 Gao, Z., H. Liu, G. G. Katul, and T. Foken, 2017: Non-closure of the surface energy balance
572 explained by phase difference between vertical velocity and scalars of large atmospheric
573 eddies. *Environ. Res. Lett.*, **12**, <https://doi.org/10.1088/1748-9326/aa625b>.
- 574 Guo, H., Li, S., Wong, F. L., Qin, S., Wang, Y., Yang, D., & Lam, H. M. (2021). Drivers of
575 carbon flux in drip irrigation maize fields in northwest China. *Carbon Balance and*
576 *Management*, 16(1), 1–16. <https://doi.org/10.1186/s13021-021-00176-5>
- 577 Gerken, T., and Coauthors, 2018: Investigating the mechanisms responsible for the lack of
578 surface energy balance closure in a central Amazonian tropical rainforest. *Agric. For.*
579 *Meteorol.*, **255**, 92–103, <https://doi.org/10.1016/j.agrformet.2017.03.023>.
- 580 Kidston, J., Brümmer, C., Black, T. A., Morgenstern, K., Nestic, Z., McCaughey, J. H., &
581 Barr, A. G. (2010). Energy balance closure using eddy covariance above two different
582 land surfaces and implications for CO₂ flux measurements. *Boundary-Layer*
583 *Meteorology*, 136(2), 193–218. <https://doi.org/10.1007/s10546-010-9507-y>
- 584 Kole, C., 2013: *Genomics and breeding for climate-resilient crops: Vol. 2 target traits*. 1–474
585 pp.
- 586 Kottke, M., J. Grieser, C. Beck, B. Rudolf, and F. Rubel, 2006: World map of the Köppen-
587 Geiger climate classification updated. *Meteorol. Zeitschrift*, **15**, 259–263,
588 <https://doi.org/10.1127/0941-2948/2006/0130>.
- 589 Leclerc, M. Y., and T. Foken, 2014: *Footprints in micrometeorology and ecology*. Springer,.
- 590 Lee, X., Q. Yu, X. Sun, J. Liu, Q. Min, Y. Liu, and X. Zhang, 2004: Micrometeorological
591 fluxes under the influence of regional and local advection: A revisit. *Agric. For.*
592 *Meteorol.*, **122**, 111–124, <https://doi.org/10.1016/j.agrformet.2003.02.001>.
- 593 Leuning, R., E. van Gorsel, W. J. Massman, and P. R. Isaac, 2012: Reflections on the surface

- 594 energy imbalance problem. *Agric. For. Meteorol.*, **156**, 65–74,
595 <https://doi.org/10.1016/j.agrformet.2011.12.002>.
- 596 Malhi, Y., K. McNaughton, and C. Von Randow, 2004: Low Frequency Atmospheric
597 Transport and Surface Flux Measurements. 101–118, [https://doi.org/10.1007/1-4020-](https://doi.org/10.1007/1-4020-2265-4_5)
598 [2265-4_5](https://doi.org/10.1007/1-4020-2265-4_5).
- 599 Manon, M., and M. Kristian, 2020: Estimating local atmosphere-surface fluxes using eddy
600 covariance and numerical Ogive optimization. **15**, 21387–21432,
601 <https://doi.org/10.5194/acpd-14-21387-2014>.
- 602 Mauder, M., and T. Foken, 2006: Impact of post-field data processing on eddy covariance
603 flux estimates and energy balance closure. *Meteorol. Zeitschrift*, **15**, 597–609,
604 <https://doi.org/10.1127/0941-2948/2006/0167>.
- 605 Medrano, H., and Coauthors, 2015: From leaf to whole-plant water use efficiency (WUE) in
606 complex canopies: Limitations of leaf WUE as a selection target. *Crop J.*, **3**, 220–228,
607 <https://doi.org/10.1016/j.cj.2015.04.002>.
- 608 Meyers, T. P., & Hollinger, S. E. (2004). An assessment of storage terms in the surface energy
609 balance of maize and soybean. *Agricultural and Forest Meteorology*, 125(1–2), 105–115.
610 <https://doi.org/10.1016/j.agrformet.2004.03.001>
- 611 Oncley, S. P., and Coauthors, 2007: The energy balance experiment EBEX-2000. Part I:
612 Overview and energy balance. *Boundary-Layer Meteorol.*, **123**, 1–28,
613 <https://doi.org/10.1007/s10546-007-9161-1>.
- 614 Peddinti, S. R., Kambhammettu, B. V. N. P., Rodda, S. R., Thumaty, K. C., & Suradhaniwar,
615 S. (2020). Dynamics of Ecosystem Water Use Efficiency in Citrus Orchards of Central
616 India Using Eddy Covariance and Landsat Measurements. *Ecosystems*, 23(3), 511–528.
617 <https://doi.org/10.1007/s10021-019-00416-3>
- 618 Rahman, M. M., Zhang, W., & Wang, K. (2019). Assessment on surface energy imbalance and
619 energy partitioning using ground and satellite data over a semi-arid agricultural region in
620 north China. *Agricultural Water Management*, 213(June 2018), 245–259.
621 <https://doi.org/10.1016/j.agwat.2018.10.032>
- 622 Reed, D. E., J. M. Frank, B. E. Ewers, and A. R. Desai, 2018: Time dependency of eddy
623 covariance site energy balance. *Agric. For. Meteorol.*, **249**, 467–478,

- 624 <https://doi.org/10.1016/j.agrformet.2017.08.008>.
- 625 Sakai, R. K., D. R. Fitzjarrald, and K. E. Moore, 2001: Importance of low-frequency
626 contributions to eddy fluxes observed over rough surfaces. *J. Appl. Meteorol.*, **40**, 2178–
627 2192, [https://doi.org/10.1175/1520-0450\(2001\)040<2178:IOLFCT>2.0.CO;2](https://doi.org/10.1175/1520-0450(2001)040<2178:IOLFCT>2.0.CO;2).
- 628 Sharma, B. R., Gulati, Mohan, Gayathri, Manchanda, S., Ray, I., & Amarasinghe, U. (2018).
629 Water Productivity Mapping of Major Indian Crops. NABARD and ICRIER, 4(1), 88–
630 100.
- 631 Shankar, V., C. S. P. Ojha, and K. S. H. Prasad, 2012: Irrigation Scheduling for Maize and
632 Indian-mustard based on Daily Crop Water Requirement in a Semi- Arid Region. **6**,
633 476–485.
- 634 Soujanya, B., B. B. Naik, M. U. Devi, T. L. Neelima, and A. Biswal, 2021: Dry Matter
635 Production and Nitrogen Uptake as Influenced by Irrigation and Nitrogen Levels in
636 Maize. *Int. J. Environ. Clim. Chang.*, 155–161,
637 <https://doi.org/10.9734/ijecc/2021/v11i1130528>.
- 638 Sun, X. M., Z. L. Zhu, X. F. Wen, G. F. Yuan, and G. R. Yu, 2006: The impact of averaging
639 period on eddy fluxes observed at ChinaFLUX sites. *Agric. For. Meteorol.*, **137**, 188–
640 193, <https://doi.org/10.1016/j.agrformet.2006.02.012>.
- 641 Tang, X., Z. Ding, H. Li, X. Li, J. Luo, J. Xie, and D. Chen, 2015: Characterizing ecosystem
642 water-use efficiency of croplands with eddy covariance measurements and MODIS
643 products. *Ecol. Eng.*, **85**, 212–217, <https://doi.org/10.1016/j.ecoleng.2015.09.078>.
- 644 Tong, X., J. Zhang, P. Meng, J. Li, and N. Zheng, 2014: Ecosystem water use efficiency in a
645 warm-temperate mixed plantation in the North China. *J. Hydrol.*, **512**, 221–228,
646 <https://doi.org/10.1016/j.jhydrol.2014.02.042>.
- 647 Tong, X. J., J. Li, Q. Yu, and Z. Qin, 2009: Ecosystem water use efficiency in an irrigated
648 cropland in the North China Plain. *J. Hydrol.*, **374**, 329–337,
649 <https://doi.org/10.1016/j.jhydrol.2009.06.030>.
- 650 Twine, T. E., and Coauthors, 2000: Correcting eddy-covariance flux underestimates over a
651 grassland. *Agric. For. Meteorol.*, **103**, 279–300, [https://doi.org/10.1016/S0168-](https://doi.org/10.1016/S0168-1923(00)00123-4)
652 1923(00)00123-4.
- 653 Vickers, D., & Mahrt, L. (1997). Quality control and flux sampling problems for tower and

- 654 aircraft data. *Journal of Atmospheric and Oceanic Technology*, 14(3), 512–526.
655 [https://doi.org/10.1175/1520-0426\(1997\)014<0512:QCAFSP>2.0.CO;2](https://doi.org/10.1175/1520-0426(1997)014<0512:QCAFSP>2.0.CO;2)
- 656 Wang, X., C. Wang, and B. Bond-Lamberty, 2017: Quantifying and reducing the differences
657 in forest CO₂-fluxes estimated by eddy covariance, biometric and chamber methods: A
658 global synthesis. *Agric. For. Meteorol.*, **247**, 93–103,
659 <https://doi.org/10.1016/j.agrformet.2017.07.023>.
- 660 Wilson, K., E. Falge, M. Aubinet, and D. Baldocchi, 2002: DigitalCommons @ University of
661 Nebraska - Lincoln Energy Balance Closure at FLUXNET Sites. *Agric. For. Meteorol.*,
662 223–243.
- 663 Zhang, P., G. Yuan, and Z. Zhu, 2013: Determination of the averaging period of eddy
664 covariance measurement and its influences on the calculation of fluxes in desert riparian
665 forest. *Arid L. Geogr.*, **36**, 401–407.
- 666
- 667